Composites Part B 80 (2015) 20–26

Contents lists available at ScienceDirect

Composites Part B

journal homepage: www.elsevier.com/locate/compositesb

Study of the reinforcing mechanism and strain sensing in a carbon black filled elastomer

G. Georgousis [a], C. Pandis [b], C. Chatzimanolis-Moustakas [b], A. Kyritsis [b], E. Kontou [a, *], P. Pissis [b], J. Krajči [c], I. Chodák [c], J. Tabačiarová [c], M. Mičušík [c], M. Omastová [c]

[a] Mechanics Department, National Technical University of Athens, Iroon Polytechniou 9, Zografou, 15780, Athens, Greece
[b] Physics Department, National Technical University of Athens, Iroon Polytechniou 9, Zografou, 15780, Athens, Greece
[c] Polymer Institute, Slovak Academy of Sciences, Dúbravska cesta 9, 845 41, Bratislava 45, Slovakia

ARTICLE INFO

Article history:
Received 4 February 2015
Received in revised form
7 April 2015
Accepted 13 May 2015
Available online 21 May 2015

Keywords:
B. Electrical properties
B. Mechanical properties
A. Nano-structures

ABSTRACT

The mechanical and electrical properties of a styrene-butadiene rubber (SBR) matrix reinforced with carbon black, at various weight fractions were experimentally studied. The electroconductive composites were used for strain sensing, under tension, by measuring together strain and electrical resistance. The storage and loss modulus decrement with strain were also investigated, on the basis of Payne effect, while a micromechanical model developed elsewhere was employed for the interpretation of the reinforcing mechanism of the composites examined.

1. Introduction

The reinforcing mechanism of polymeric structure due to the presence of nanofillers, in spite of a large number of research works, is still a matter of great interest, especially at temperatures above glass transition temperature Tg, where melts and elastomers are also involved [1,2]. The effect of nanofillers on the mechanical performance as well as on the nonlinear viscoelastic response represents an issue of great importance, that needs to be further explored. A detailed presentation of theories attributing the nonlinear viscoelastic behaviour on filler agglomeration and network formation has been reported by Heinrich et al. [3]. According to these theories, the mechanical enhancement is due to the formation of filler structures, while the reinforcement decrement with increasing strain is assigned to the damage of these structures. Moreover, the effect of strain amplitude on the dynamic viscoelastic properties of carbon black filled elastomers, has been known for many decades, but it was distinguished by the work of Payne [4] and therefore this effect has been referred to as the Payne effect. In particular, the nonlinearity, with varying strain, of the dynamic mechanical properties elastomers filled with carbon black, has been the subject of previous works [5–9]. The Payne effect is of particular importance for a variety of applications, especially in tire industry, because the nonlinearity it refers to is in the strain range applicable in tire operations. Payne [9] has concluded that the nonlinear behaviour of filled vulcanized elastomers is rooted in the breakdown of carbon black network structure, and the energy involved in this breakdown comes from the van der Waals forces between the carbon black particles. Similar ideas have been proposed in previous works [5,7]. Later this interpretation however, has been questioned by several researchers [10,11], given that Payne effect is also observed at low filler loadings, where the inter-aggregate distances are beyond the range of van der Waals forces. Moreover, the viscoelastic nature of Payne effect could not be described by the proposed mechanism. In view of this, Sternstein and Zhu [1] introduced a new theory to account for the Payne effect. According to their analysis, temporary bonding of molecular chains to the filler surface result in trapped entanglements, affecting the mobility and conformational freedom of both near- and far-field matrix chains. In other words, the presence of entanglements, due to the long polymer chains, existing above Tg, has a strong effect on the material's viscoelastic behaviour. Among the large number of works discussing the Payne effect, physical models providing a quantitative description were

* Corresponding author.
E-mail address: ekontou@central.ntua.gr (E. Kontou).

http://dx.doi.org/10.1016/j.compositesb.2015.05.021
1359-8368/

presented by Kraus [12], Heinrich-Klüppel [13], Huber and Vilgis [14], while pure empirical mathematical models are presented in work of Dean et al. [15]. The mechanical enhancement of polymers, polymer melts and elastomers emerges from a variety of fillers and nanofillers, such as carbon black, carbon nanotubes, and graphene. Apart from the reinforcing effect, a common characteristic of the above-mentioned fillers is that when they have been implanted into an insulating polymer matrix, an electrically conductive polymer composite is obtained. Therefore, the intrinsic conductivity of these fillers makes them multifunctional and suitable for a wide variety of applications such as their usage as sensors for strain sensing for structural health monitoring [16]. The main concept is using the structural material itself as the sensor. This concept is also referred to as self-sensing and has the advantages of being low-cost, it can be applied to a large volume of the structural material and there is an absence of mechanical property loss. The concept is based on the monitoring of the changes in electrical conductivity in order to detect the onset, nature and evolution of dangerous deformation levels in advanced polymer-based composites. A lot of research on such nanocomposites under mechanical loading has been done concerning electrical measurements such as resistivity or capacitance to examine their potential use in deformation or pressure sensors [17–19]. The relationship between conductivity and stress-strain curve has been studied for two different matrices, thermoplastic and elastomeric, reinforced with carbon black [19], however, little attention has been paid to the mechanical enhancement of these materials and the related mechanisms.

The aim of the present work is twofold; first to study the reinforcing mechanism of carbon black filler in SBR elastomer, and the dynamic modulus decrement with strain amplitude within the context of hydrodynamic and micro-mechanics models, and second to examine the effect of the filler content on the electrical properties of SBR/nanocomposite, and its performance for strain sensing. Regarding reinforcing effect, the Young's modulus of the SBR nanocomposites has been described by well known equations, while the storage modulus decrement with strain has been elaborated on the basis of the existence of a filler network. It was found that the network junction model [11] describes better the reinforcing effect of the SBR/nanocomposite. Therefore, this model has been employed for the additional interpretation of the Payne effect. An additional interesting point is that the mode of deformation applied in our dynamic mechanical testing is the tensile one, unlike shear strain used in the majority of previous relevant works. The present work gives a further insight into the relationship between the filler structures, as well as the polymer dynamics in the interfacial region (between carbon black and elastomer), contributing this way to the interpretation of the reinforcing mechanism of the elastomeric matrix. Hereafter, the sensing behaviour of the SBR/nanocomposites has been thoroughly examined, in relation to the carbon black content.

2. Experimental part

2.1. Materials

The elastomeric material employed as a matrix was poly(styrene-co-butadiene) rubber (SBR, Unipetrol Group, Kralupy nad Vltavou, Czech Republic), which was produced by cold emulsion polymerization, and had a styrene content of 22.5–24.5 wt%, an antioxidant content of 1–1.75 wt%, an organic acid content of 5.0–6.5 wt%, and a Mooney viscosity (1 + 40 at 100 °C) of 47–56. SBR matrix was reinforced by carbon black (CB) of type Chezacarb A (Unipetrol RPA, Litvinov, Czech Republic), as a superconductive carbon black. The matrix was reinforced with 2, 5 10, 15 and 20 wt% of carbon black.

2.2. In situ electrical measurements upon tensile loading

The samples were subjected to tensile loading using an Instron 1121 tester. For each filler content at least three samples were measured. The specimen's gauge length was 20 mm, while the cross-section area was 1–2 mm in thickness and 4 mm wide. The crosshead speed was 10 mm/min. A scheme of the experimental setup is depicted in Fig. 1. A non-contact experimental method, based on a laser extensometer was employed for detailed strain measurement [20]. The maximum value of strain applied during the tensile experiments was 60% for materials. Higher strain values attained by the elastomeric material was not possible to be tested by this method.

During each experiment the electrical resistance along the gauge length of each specimen was monitored to observe the electrical behaviour of the material under mechanical deformation. For that reason, the tensile stress, the longitudinal strain and the electrical resistance as a function of time were measured simultaneously.

For the electrical measurements a Keithley Source-Meter 2400 was used. At each measurement a fixed direct current (DC) was applied to the two electrical contacts while the voltage drop between them was measured. For that reason, golden stripes had been sputtered on the surface of each sample, as shown in Fig. 1a, where copper cables were glued using electrically conductive glue. Then the relative change of the resistance ($\Delta R/R_0$) as a function of time was calculated, where R_0 is the resistance at the beginning of the measurement. Finally, the stress and the $\Delta R/R_0$ were plotted against strain. Electrical conductivity and percolation threshold was studied by dielectric relaxation spectroscopy (DRS) measurements in the frequency range 10^{-1}–10^{6} Hz at room temperature using an Alpha analyzer (Novocontrol). Golden electrodes were sputtered on both sides of round sample to assure good electrical contact between these and the gold-plated capacitor plates. Further details about the method can be found in our previous publications (e.g. Ref. [21]).

2.3. Dynamic mechanical analysis

Dynamic Mechanical Analysis (DMA) experiments were performed using the TA Instruments DMA Q800 instrument. The mode of deformation applied was tension, and the mean dimensions of

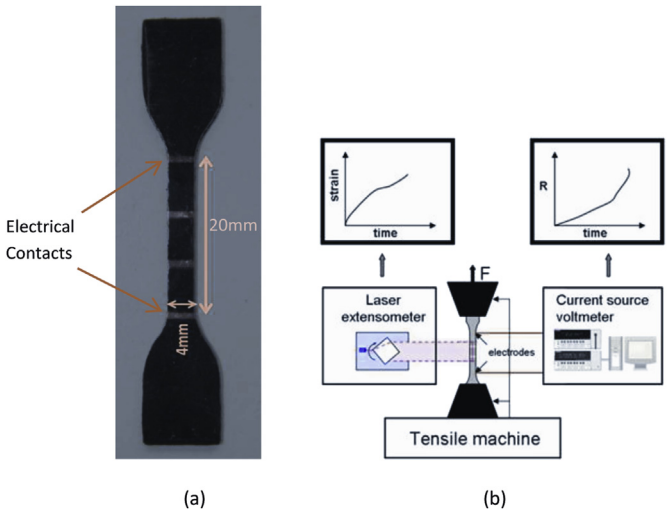

Fig. 1. (a) Picture of the sample with the golden stripes, (b) Experimental setup. (For interpretation of the references to colour in this figure legend, the reader is referred to the web version of this article.)

specimens were 2.9 mm × 2 mm × 17.5 mm (width × thickness × length). The experiments were performed at room temperature, which is above the glass transition of the elastomeric matrix temperature, at four frequency values of 1, 5, 10 and 15 Hz. A strain-sweep procedure has been followed, and the storage, loss modulus and tanδ with varying strain were recorded.

3. Results and discussion

3.1. Dynamic moduli dependence on strain amplitude

The effects of strain on storage E′ and loss E′′ modulus is illustrated in Figs. 2 and 3 respectively, at frequency equal to 10 Hz, for neat rubber matrix and its composites with varying carbon black weight fraction. The neat SBR exhibits linear viscoelastic behavior in the strain range examined. Regarding SBR/nanocomposites, a gradual decrement in storage and loss modulus with increasing strain is observed. Similar graphs were obtained at 1, 5, and 15 Hz. It has been found that with increasing frequency, a decrease was observed in the strain values where the onset of nonlinearity occurs. On the other hand, at constant frequency, the strain where nonlinearity starts is reduced with increasing filler content, while in general, the degree of nonlinearity increases with filler concentration. In Fig. 2 it is shown that at high strain region the storage modulus converges to some certain terminal value, but it was impossible to attain this due to the force limitation imposed by the DMA device employed. Regarding the loss modulus dependence on strain (Fig. 3) a quite similar to the storage modulus response is obtained, at all frequency values examined. Comparing the two plots, it is revealed that in both, low strain and high strain range, the difference in storage modulus values with increasing filler content is much higher than the corresponding values of the loss modulus.

Payne [4] has shown that the maximum value of loss modulus varies linearly with the difference between low and high amplitude storage modulus. Following our results, the corresponding plot is illustrated in Fig. 4, and for each frequency examined the data lie on a single curve. Therefore, a behavior similar to other filled elastomers is revealed, which can be expressed by the following empirical equation:

$$E''_{max} = a + b(E'_0 - E'_\infty) \quad (1)$$

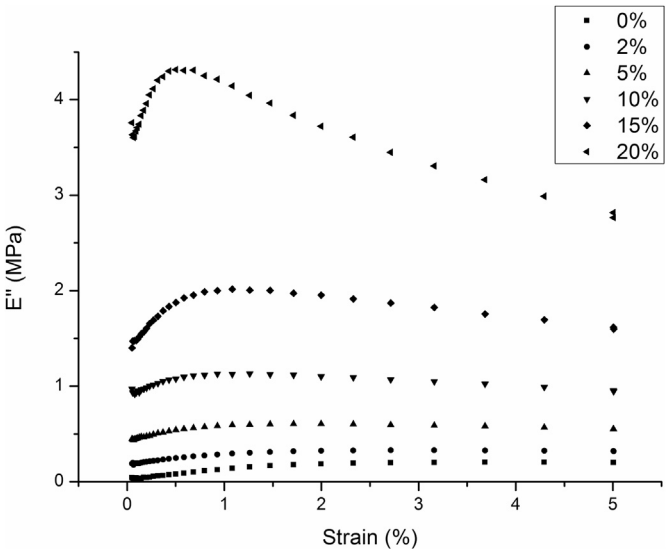

Fig. 3. Longitudinal loss modulus versus strain at room temperature and 10 Hz for SBR filled with various contents of carbon black.

where E''_{max} is the maximum value of loss modulus, E'_0 the storage modulus at the initial low strain region, E'_∞ the storage modulus at the high strain region, *a* and *b* parameters that need to be estimated. The experimental points at the four frequencies examined in Fig. 4, are plotted in comparison with the linear fitting of equation (1). Despite the small differences, it can be observed that all material types follow a linear dependence for each frequency value. After applying a linear fit procedure of equation. (1) in respect to the experimental data, parameter *a, b* values were found to be in average 0.33 and 0.39 correspondingly.

According to work of Heinrich et al. [13], this plot reveals a relationship between storage and loss modulus, showing that the mechanism for the change in storage modulus and loss peak with strain are related. Therefore, this linear relationship provides an evidence of a loss mechanism of agglomeration-deagglomeration, as reported by Kraus [12]. Later, this loss mechanism has been related to the breaking and remaking of contacts between filler particles or fillers and bulk matrix. Therefore, additional strain energy is dissipated [22]. Kraus developed a quantitative model to

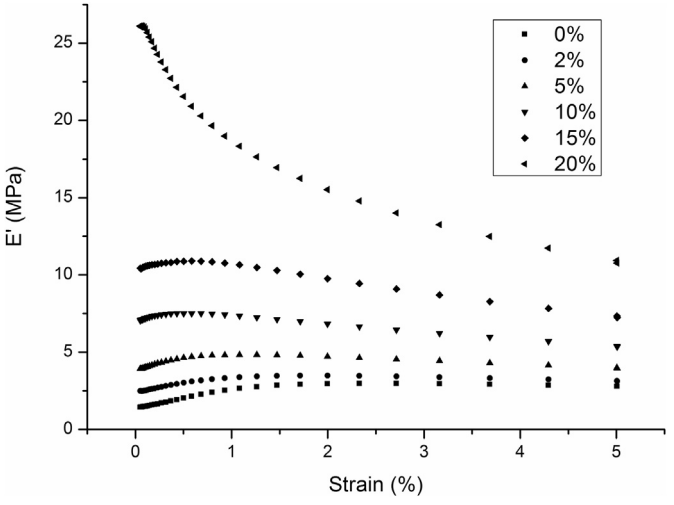

Fig. 2. Longitudinal storage modulus versus strain at room temperature and 10 Hz for SBR filled with various contents of carbon black.

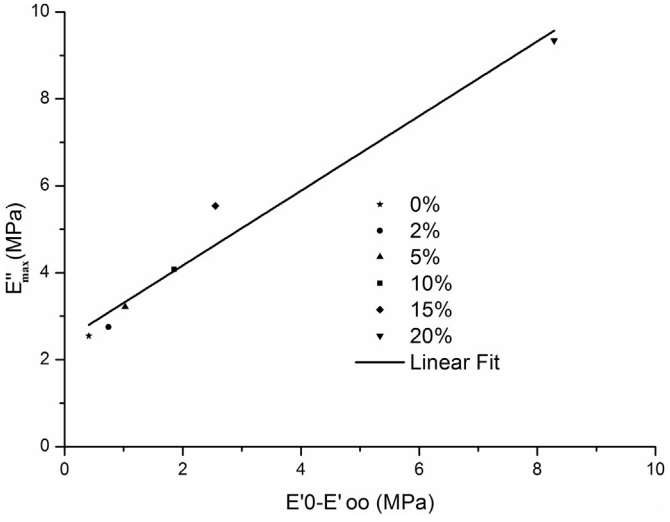

Fig. 4. Payne plot for all SBR/carbon black composites, at 10 Hz.

analyze the Payne's effect, based on the agglomeration/deagglomeration of carbon black agglomerates. According to this model, the excess modulus $E' - E'_\infty$ of the agglomeration network is proportional to the existing number of carbon-carbon contacts:

$$\frac{E'-E'_\infty}{E'_0 - E'_\infty} = \frac{1}{1+\left(\varepsilon/\varepsilon_c\right)^{2m}} \tag{2}$$

Where E' is the storage modulus at strain ε and ε_c is the strain where the quantity $E' - E'_\infty$ has decreased to half of its zero strain value, m is an empirical constant.

Moreover, Kraus [12] proposed that the loss mechanism is caused by the additional forces between carbon particles or between carbon particles and matrix, during the breaking of contacts. Therefore he concluded that the excess loss modulus $E''-E''_\infty$ is given by:

$$E'' - E''_\infty = \frac{C\varepsilon^m (E'_0 - E'_\infty)}{1+\left(\frac{\varepsilon}{\varepsilon_c}\right)^{2m}} \tag{3}$$

where C is a constant that needs to be fitted. The correlation of equations (2) and (3) with the experimental data was fairly good for all materials in the low strain region, and is shown representatively for 20% CB in Figs. 5 and 6 supporting by such a way the mechanism proposed by Kraus. The deviation obtained at higher strain values may indicate that the agglomeration-deagglomeration mechanism is limited to the low strain region. It should also be pointed out that our experimental data are obtained by the tensile mode of deformation, unlike to the shear deformation employed in previous works [13]. Parameter values were fitted as: $C = 1.8$, $m = 0.4$ and $\varepsilon_c = 0.005$. The estimation of parameters involved in equation. (3) has been performed by a non-linear fit procedure, using the software Mathematica.

3.2. Young's modulus variation with carbon black content

The description of the reinforcement effect on the Young's modulus can be done with either the Einstein [23] equation (4), valid at low filler content:

$$E = E_m\left(1 + 2.5v_f\right) \tag{4}$$

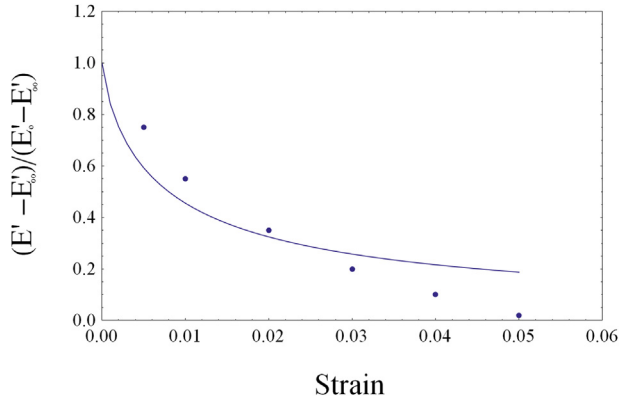

Fig. 5. Strain variation of $E' - E'_\infty / E'_0 - E'_\infty$ for SBR reinforced with 20% carbon black.

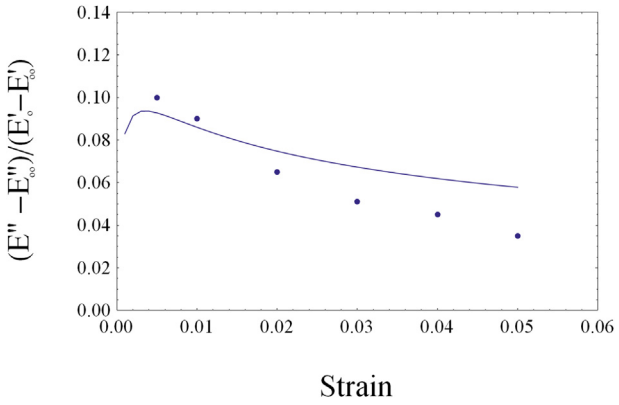

Fig. 6. Strain variation of $E'' - E''_\infty / E'_0 - E'_\infty$ for SBR reinforced with 20% carbon black.

where E and E_m is the Young's modulus of the composite and matrix correspondingly, and V_f is the filler volume fraction, or the Guth and Gold equation (5) [24] for higher filler loadings:

$$E = E_m\left(1 + 2.5v_f + 14.1v_f^2\right) \tag{5}$$

Due to the inability of these equations to satisfactorily describe the reinforcing effect of carbon black-elastomers, attempts to improve equation (5) were presented in a previous work [11]. The main concept of these approaches was to introduce a larger effective volume fraction $V_{f_{eff}}$, in order to fit the experimental data more precisely [25–27]. Kraus proposed the following expression for the calculation of the effective volume fraction:

$$\frac{V_{f_{eff}}}{V_f} = 1 + \frac{CDBP - 31}{55} \tag{6}$$

Where CDBP is a measure of the void volume in c.c. for 100 gm of crushed carbon black, in our case equal to 340 c.c/100g.

In Fig. 7, the experimentally obtained normalized modulus E/E_m is plotted versus carbon black volume fraction, together with the theoretical curves of equations (4)–(6). The volume fraction V_f has been calculated as the half of the corresponding weight fraction [2,19]. From Fig. 7 it is extracted that the normalized modulus of the SBR composites examined cannot be described by the Einstein and

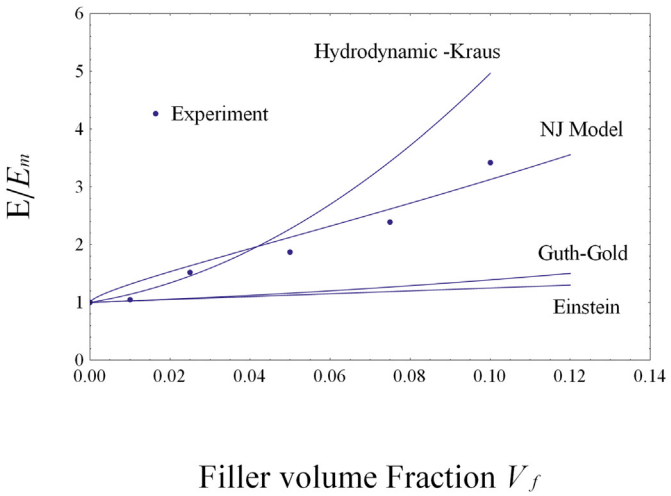

Fig. 7. Normalized Young's modulus with varying carbon black volume fraction for the SBR/carbon black composites.

Guth–Gold equations (4) and (5) respectively. On the other hand, according to Kraus approach [26], and employing a higher $V_{f_{eff}}$, a better approximation to the experimental data is obtained at low carbon black volume fractions, followed hereafter by a deviation. Considering this result, a different treatment will be applied, in terms of a micro-mechanics model [11].

As mentioned in Ref. [13] the mechanism of filler network breakdown and reformation can adequately describe the modulus decrement with strain. Regarding however the Young's modulus enhancement, the energy dissipation process, and hysteresis effects observed in filled elastomers, additional assumptions need to be made. In view of this, the network junction model is focused on the study of the energy dissipation process in junction points between filler aggregates [22]. This was further developed to describe the modulus increment with filler volume fraction. This network junction model takes into account the filler morphology and suggests that under the extensional mode, rubber molecular chain friction in the junction region, instead of filler-rubber interfacial slippage could be the dominant mechanism of energy dissipation under small strain cycle conditions. On this basis, a simple nanocomposite model formulating the reinforcing effect of carbon black was introduced [11,22]. According to this model, in an initial tight carbon black network, rubber is added until a normal loading is achieved. During this stage, the network junctions width is widened from zero to a characteristic width h. To calculate the Young's modulus, a cubic sample with 1 cm sides is considered, and the average number of aggregates in the cross-sectional area of one square centimeter can be evaluated. Hereafter, the force and displacement between two rigid spheres [28] are calculated, and the total network junction's contribution to the modulus is evaluated. This expression combined with the matrix rubber contribution to the modulus of the composite material, results to the following equation for the modulus of the filled rubber as suggested by Ouang [11]:

$$E = 1.39\alpha E_m\left[6v_f/(\pi\eta_p)\right]^{1.9/3}\left[1-\left(v_f/v_{f_{max}}\right)^{1/3}\right]^{-0.9} + E_m\left(1-v_f^{2/3}\right) \quad (7)$$

Where α is a constant, and η_p the average number of primary particles per aggregate. The quantity $v_{f_{max}}$ denotes the maximum carbon black volume fraction, when network junctions width h becomes zero and is given by:

$$v_{f_{max}} = \frac{100/\rho}{[CDBP + 100/\rho]} \quad (8)$$

Where ρ is the carbon black's apparent density, equal to 0.115 g/cm^3. Parameters α and η_p were fitted to take the values 6 and 4 respectively, while $V_{f_{max}}$ was calculated equal to 0.719. The calculation of parameters α and η_p, has been performed with a non linear fit procedure, in terms of a program with the software Mathematica. Following Fig. 7, the best correlation with the experimental data is achieved by the network junction model of equation (7).

3.3. Electrical properties – In situ electrical measurements upon tensile loading

The electrical properties of the prepared samples as well as the electrical percolation threshold were studied using dielectric relaxation spectroscopy (DRS). Fig. 8 shows the frequency (f) dependence of the real part of the complex electrical conductivity, $\sigma'(f)$, measured at room temperature for the virgin SBR and the composites containing various carbon black contents. AC (Alternating Current) conductivity is frequency dependent in the whole frequency range for the pure SBR and for composites with CB content up to 5 wt.%, a typical behaviour of insulating materials. In contrary, for the composites with filler content higher than 10 wt % a flat DC (Direct Current) response invariant of frequency is obtained. This independence from frequency, which is characteristic for conductive materials, is extended in the whole frequency range. The AC conductivity measurements clearly show that the transition from the insulating to the conducting phase, the so-called percolation threshold (p_c), is observed between 5 and 10 wt.% CB, followed by a sharp increase in conductivity of almost nine orders of magnitude. For the exact calculation of p_c the well known scaling law from percolation theory [29] was applied:

$$\sigma = \sigma_{dc}(p - p_c)^t \quad (9)$$

where σ_{dc} is the DC conductivity, p is the volume fraction of the filler, and t is a critical exponent related with the dimensionality of the investigated system. The best fit was obtained for $p_c = 7.0 \pm 0.2$ wt% or 3.5 ± 0.1 vol% and $t = 5.7 \pm 0.2$ which is a close value with the one defined in Ref. [19] for the same SBR/carbon black composites. For the above evaluation the wt.% values were primary converted to vol% as described in Ref. [30].

The stress-strain results, plotted together with the relative resistance $\Delta R/R_0$ for samples SBR with 15 and 20% wt in CB are illustrated in Figs. 9 and 10 correspondingly. The increase of $\Delta R/R_0$ with strain could be explained as a result of destruction of percolating paths forming the conducting network [16,21]. The results concerning electrical measurements show that the curve for relative resistance change increases linearly as the elongation proceeds, for both material types examined. This linearity was observed even for high strain rates such as 50%. For 15 wt% filler content the initial resistance was 12 kΩ and the slope is 3, which corresponds to a 75° angle. Samples with 20 wt% carbon black content showed an initial resistance of 800 Ω and a slope of 2.6, which corresponds to an angle of 69°. The quantity $GF = \frac{\Delta R/R_0}{\varepsilon}$ is referred to in bibliography as the gauge factor [31], and can be derived from the slope of the dashed lines in Figs. 9 and 10. From these results prepared SBR/nanocomposites appear promising for use for strain sensing applications including self-sensing.

For a better understanding of the effect of strain on the electrical properties of the nanocomposites, the relative resistance change has been plotted versus strain, during a cyclic loading procedure, performed at a maximum strain 15%. In Fig. 11, a representative plot

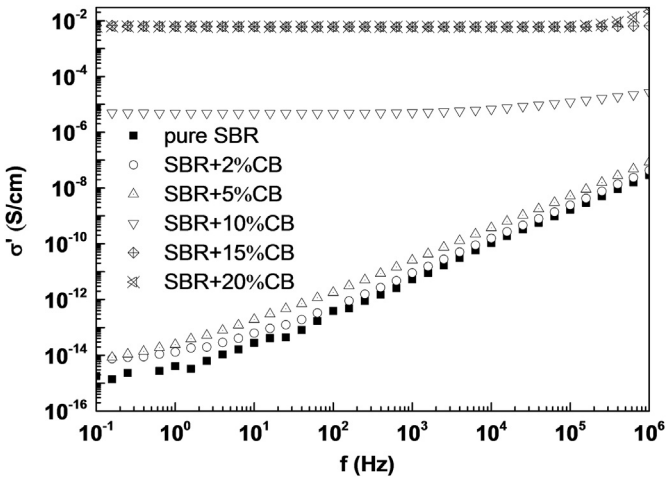

Fig. 8. Real part of conductivity σ′ against frequency measured at room temperature.

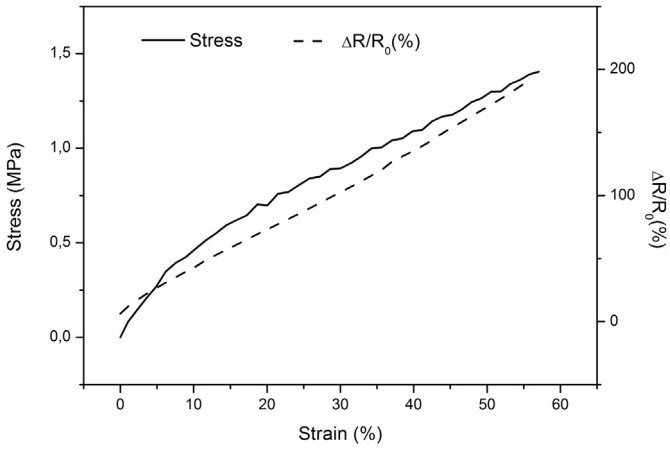

Fig. 9. Stress and Relative Resistance Change as a function of Strain for SBR/15% carbon black.

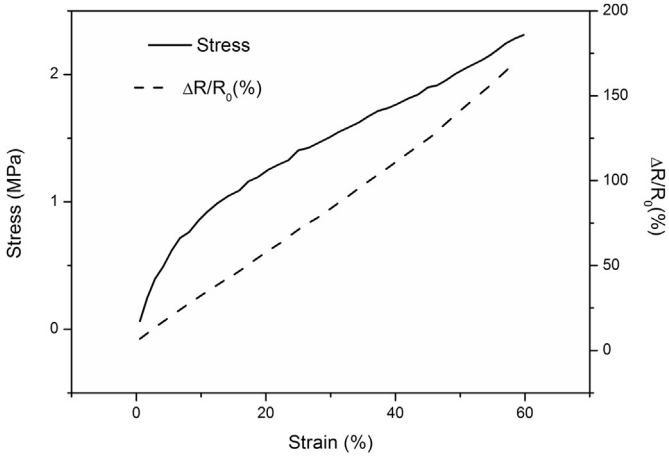

Fig. 10. Stress and Relative Resistance Change as a function of Strain for SBR/20% carbon black.

for SBR/15%CB of $\Delta R/R_0$ against strain at first and second stretching cycle (after unloading) is illustrated. A significant difference in resistance between the first and second stretching is observed. In the subsequent cycles there is repeatable recovery of the resistance

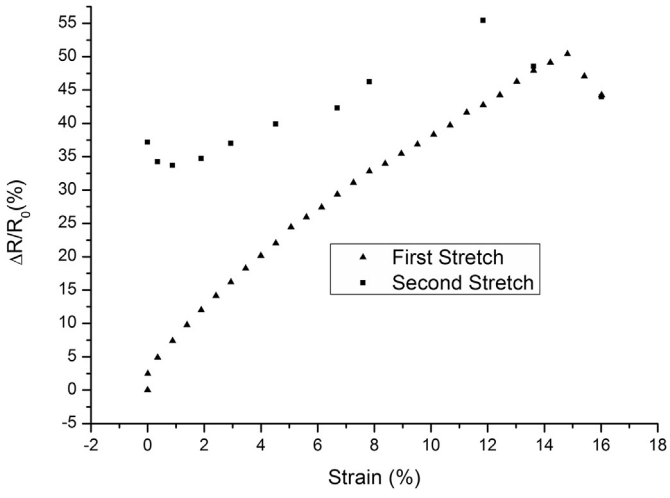

Fig. 11. Electrical resistance variation with strain for SBR/15%wt carbon black for the first and second cycle.

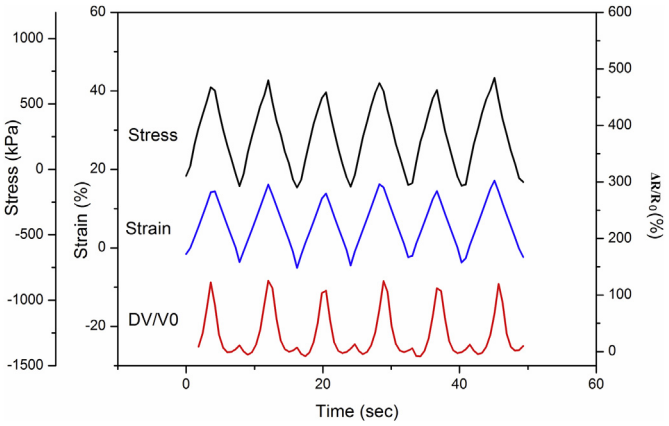

Fig. 12. Stress, Strain and Electrical resistance variation with time for SBR/15%wt carbon black for the third to sixth six cycle.

as shown in Fig. 12. The above behavior has been reported previously in SBR/carbon nanotube composites [32] as well as in SBR/carbon black composites [33] and is attributed to the fact that the filler network is not reformed after the removal of stress during the first loading–unloading cycle. It should be noted that in our case this behavior is observed at much lower strains for the composite with 15%CB. This filler content is above the percolation threshold but not very far from it, making the nanocomposite sensitive enough to monitor low strain changes, because a relatively low strain change can result in a more significant alteration of resistance change. It is generally accepted that the higher sensitivities observed for filler contents close to the percolation threshold is attributed to the more prominent changes of the sparse filler network [20,34]. The breakage of a contact in a sparse network has a higher impact on the electrical resistance than if happened in a dense network. On the other hand, the full recovery of the destructed network upon unloading is much less likely in a sparse network.

4. Conclusions

The reinforcing effect of carbon black on the SBR matrix has been modeled with a hydrodynamic model and a micromechanics one, the so-called network junction model. In both, the carbon black network effect is considered, but in the former a filler network breakdown is assumed, while in the latter the rubber junctions between aggregates seem to play a decisive role. It has been shown that for the specific SBR matrix and carbon black studied, the Young's modulus is adequately described by the network junction model for all carbon black loadings. Regarding the Payne effect, the network junction model offers only qualitative description, while the agglomeration-deagglomeration mechanism between filler aggregates was found to work well at low strain values. It was also shown that strain change and resistance change have a linear relationship. Therefore the prepared SBR/nanocomposites appear promising for use for strain sensing applications including self-sensing, as it is easy to calculate strain by measuring the relative resistance $\Delta R/R_0$ and dividing it by the slope, which can be found by proper preliminary measurements and calibration.

Acknowledgments

The research was financed by the Greek General Secretariat of Research and Technology and the Slovak Research and Development Agency in the frame of bilateral cooperation between

Slovakia and Greece (APVV SK-GR-0029-11). This work was partly financially supported by project VEGA 2/0149/14 and VEGA 2/0108/14 (Slovakia).

References

[1] Sternstein SS, Zhu Ai-Jun. Reinforcement mechanism of nanofilled polymer melts as elucidated by nonlinear viscoelastic behavior. Macromolecules 2002;35:7262–73.
[2] Zhu Ai-Jun, Sternstein SS. Nonlinear viscoelasticity of nanofilled polymers: interfaces, chain statistics and properties recovery kinetics. Comp Sci Techn 2003;63:113–26.
[3] Heinrich G, Klüppel M. Recent advances in the theory of filler networking in elastomers. Adv Polym Sci 2002;160:1–44.
[4] Payne AR. The dynamic properties of carbon black –loaded natural rubber vulcanizates. Part I. J Appl Polym Sci 1962;6:57–63.
[5] Waring IRS. Trans IR.I 1950;26:4.
[6] Fletcher WP, Gent AN. Trans IR.I 1953;29:266.
[7] Gui KE, Wilkinson CS, Gehman SD. Vibration characteristics of tread stocks. Ind Engng Chem 1952;44:720–3.
[8] Payne AR. Dynamic properties of PBNA-natural rubber vulcanizates. J Appl Polym Sci 1967;11:383–7.
[9] Payne AR. Ch. 3. In: Kraus G, editor. Dynamic properties of filler loaded rubbers in “Reinforcement of elastomers”. Wiley, N.York: Interscience Publishers; 1965.
[10] Funt J. Dynamic testing and reinforcement of rubber. Rubber Chem Techn 1988;61:842–65.
[11] Ouang GB. Modulus, hysteresis and the payne effect. Constr Simul 2006:332–43.
[12] Kraus G. Mechanical losses in carbon-black filled rubbers. J Appl Polym Sci Appl Polym Symp 1984;39:75.
[13] Heinrich G, Klüppel M. Advances in polymer science, vol. 160. Heidelberg: Springer Verlag Berlin; 2002.
[14] Huber G, Vilgis TA. Advances in polymer science, 52. Heidelberg: Springer Verlag Berlin; 1999. p. 102. Kautsch Gummi Kunstst.
[15] Dean GD, Duncan JC, Johnson AF. Determination of non-linear dynamic properties of carbon filled rubbers. Polym Test 1984;4:225.
[16] Schulte K, Baron C. Load and failure analyses of CFRP laminates by means of electrical resistivity measurements. Comp Sci Techn 1989;36(11):63–76.
[17] Knite M, Teteris V, Kiploka A, Kaupuzs J. Polyisoprene –Carbon black nanocomposites as tensile strain and pressure sensor materials. Sensors Actuators, A: Phys 2010;A110:142–9.
[18] Yasuoka T, Shimamura Y, Todoroki A. Patch-type large strain sensor using elastomeric composite filled with carbon nanofibers. Int J Aeronaut Space Sci 2013;14(2):146–51.
[19] Krajči J, Špitálsky, Chodák I. Relationship between conductivity and stress-strain curve of electroconductive composite with SBR or polycaprolactone matrices. Eur Polym J 2014;55:135–43.
[20] Georgousis G, Pandis C, Kalamiotis A, Georgiopoulos P, Kyritsis A, Kontou E, et al. Strain sensing in polymer/carbon nanotube composites by electrical resistance measurement. Compos Part B 2015;68:162–9.
[21] Logakis E, Pandis C, Peoglos V, Pissis P, Stergiou C, Piontech J, et al. Electrical/dielectric properties and conduction mechanism in melt processed polyamide/multi- walled carbon nanotubes composites. Polymer 2009;50(21):5103–11.
[22] Ouang GB, Tokita N, Wang M-J. Paper No 108. In: ACS rubber division meeting, Cleveland Ohio; 1995.
[23] Einstein A. Ann Phys 1906;19:289.
[24] Guth E, Gold O. Phys Rev 1938;53:322.
[25] Medalia AI. J Colloid Interf Sci 1970;32:115.
[26] Kraus G. Rubber Chem Techn 1972;44:199.
[27] Wang MJ, Wolff S, Tan EH. Rubber Chem Techn 1993;66(2):178.
[28] Gent AN, Park B. Rubber Chem Techn 1986;59:77.
[29] Stauffer D, Aharony A. Introduction to percolation theory. 2nd revised ed. London: Taylor and Francis; 2003.
[30] Logakis E, Pollatos E, Pandis C, Peoglos V, Zuburtikudis I, Delides CG, et al. Structure-property relationships in isotactic polypropylene/multi-walled carbon nanotubes nanocomposites. Compos Sci Technol 2010;70(2):328–35.
[31] Kaddour AS, AI-Salehi FAR, A1-Hassani STS, Hinton MJ. Electrical resistance measurement technique for detecting failure in CFRP materials at high strain rates. Compos Sci Technol 1994;51:377–85.
[32] Bokobza L, Belin C. Effect of strain on the properties of a styrene–butadiene rubber filled with multiwall carbon nanotubes. J Appl Polym Sci 2007;105:2054–61.
[33] Yamaguchi K, Busfield JJC, Thomas AG. Electrical and mechanical behavior of filled elastomers. I. The effect of strain. J Polym Sci B: Polym Phys 2003;41:2079–89.
[34] Hu N, Karube Y, Arai M, Watanabe T, Yan C, Li Y, et al. Investigation on sensitivity of a polymer/carbon nanotube composite strain sensor. Carbon 2010;48(3):680–7.